Supporting Information: Nanosecond Pulsed Discharge for CO_2 Conversion: Kinetic Modelling to Elucidate the Chemistry and Improve the Performance

Stijn Heijkers[1] , Luca Matteo Martini[2,†], Giorgio Dilecce[3,2], Paolo Tosi[2,3] and Annemie Bogaerts[1]*

[1] Research group PLASMANT, Department of Chemistry, University of Antwerp, Universiteitsplein 1, BE-2610 Wilrijk-Antwerp, Belgium

*annemie.bogaerts@uantwerpen.be, +3232652377

[2] Dipartimento di Fisica, Università di Trento, Italy

[3] P.Las.Mi Lab NANOTEC – CNR Bari, Italy

[†] Present address: Department of Applied Physics, Eindhoven University of Technology, The Netherlands

Contents

1. Detailed description of the model

The 0D model is based on solving equation (1):

$$\frac{\partial n_s}{\partial t} = \sum_{i=1}^{j}\left[\left(a_{s,i}^{R} - a_{s,i}^{L}\right)R_i\right] \quad (1)$$

where n_s is the density of species s (in m^{-3}) , j the total number of reactions, $a_{s,i}^L$ and $a_{s,i}^R$ the stoichiometric coefficients at the left hand side and right hand side of the reaction and R_i the rate of reaction (in m^{-3} s^{-1}), given by:

$$R_i = k_i \prod_s n_s^{a_{s,i}} \quad (2)$$

where k_i is the rate constant (in m^3 s^{-1} or m^6 s^{-1} for two-body or three-body reactions, respectively) and $a_{s,i}$ was defined above. The rate constants of the heavy particle reactions are either constant or dependent on the gas temperature, whereas the rate constants of the electron impact reactions depend on the electron temperature T_e or the reduced electric field E/N (i.e., the electric field E divided by the number density of all neutral species N, usually expressed in Td = 10^{-21} V m^2). The rate constants of the electron impact reactions are generally calculated according to the following equation:

$$k_i = \int_{\varepsilon_{th}}^{\infty} \sigma_i(\varepsilon) v(\varepsilon) f(\varepsilon) d\varepsilon \quad (3)$$

with ε the electron energy (usually in eV), ε_{th} the minimum threshold energy needed to induce the reaction, $v(\varepsilon)$ the velocity of the electrons (in m s^{-1}) , $\sigma_i(\varepsilon)$ the cross section of collision i (in m^2), and $f(\varepsilon)$ the (normalized) electron energy distribution function (EEDF; in eV^{-1}) calculated using a Boltzmann solver. The reactions included in the model, along with their rate coefficients and the references where these data are adopted from, are listed in Tables S.1-S.5.

In this work we use the ZDPlaskin code [1] to solve the balance equations (1) of all species, which also has a built-in Boltzmann solver, called BOLSIG+ [2], to calculate the EEDF and the rate constants of the electron impact reactions based on a set of cross sections, the plasma composition, the gas temperature and the reduced electric field (E/N).

The electric field (E; in V m^{-1}) is calculated from a given power density, using the so-called local field approximation [3]:

$$E = \sqrt{\frac{P}{\sigma}} \quad (4)$$

with P the input power density (in W m^{-3}) and σ the plasma conductivity (A V^{-1} m^{-1}). The plasma conductivity is estimated at the beginning of the simulations as [3]:

$$\sigma = \frac{e^2 n_{e,init}}{m_e \nu_m} \quad (5)$$

with e the elementary charge (1.6022x10^{-19} C), $n_{e,init}$ the initial electron density (in m^{-3}), m_e the electron mass (9.1094x10^{-31} kg) and ν_m the collision frequency (in s^{-1}) calculated using BOLSIG+. During the simulation the plasma conductivity is calculated as [3]:

$$\sigma = \frac{e v_d n_e}{(\frac{E}{N})_{prev} n_0} \quad (6)$$

with v_d the electron drift velocity (in m s^{-1}), which is calculated using BOLSIG+ implemented in ZDPlaskin, and $(\frac{E}{N})_{prev}$ the reduced electric field at the previous time step (in V m^2).

The balance equation for the gas temperature T_g (in K) is also solved:

$$N \frac{\gamma k}{\gamma - 1} \frac{dT_g}{dt} = P_{e,el} + \sum_j R_j \Delta H_j - P_{ext} \quad (7)$$

where $N = \sum n_i$ is the total neutral species density, γ is the specific heat ratio of the total gas mixture, k is the Boltzmann constant (in J K^{-1}), $P_{e,el}$ is the gas heating power density due to elastic electron-neutral collisions (in W m^{-3}), R_j is the rate of reaction j (in m^{-3} s^{-1}), ΔH_j is the heat released (or consumed when this value is negative) by reaction j (in J) and P_{ext} is the heat loss due to energy exchange with the surroundings (in W m^{-3}). The latter one is originally calculated as:

$$P_{ext} = \frac{8\lambda}{R^2}(T_g - T_{g,i}) \quad (8)$$

where λ is the gas thermal conductivity (in W m^{-1} K^{-1}), R the radius of the plasma zone, T_g the plasma gas temperature and $T_{g,i}$ the gas temperature just before the start of the pulse, i.e. 293.15 K at the beginning of the simulation, or the gas temperature at the end of the afterglow of the previous pulse (see main text for more explanation).

Greig et al.[4] and Shneider [5] showed that in ns-pulsed discharges turbulent cooling is important. Therefore, we multiply equation (8) by a factor 9 to incorporate the more effective turbulent cooling, which is also successfully applied in 0D simulations for a turbulent GAP [6–8], with this factor based on 2D fluid dynamics simulations [9].

The specific heat ratio of the total (ideal) gas mixture is calculated from the specific heat ratios of the individual species in the model, γ_i, using the formula:

$$N\frac{\gamma}{\gamma-1} = \sum_i n_i \frac{\gamma_i}{\gamma_i-1} \quad (9)$$

where n_i are the densities of the individual species i. The individual specific heat ratios, γ_i, can be calculated from the specific heat capacity at constant pressure $c_{p,i}$ (in J K^{-1} kg^{-1}) using the relation:

$$c_{p,i} = \frac{\gamma_i}{\gamma_i-1}\frac{k}{M} \quad (10)$$

where k is the Boltzmann constant and M is the molar weight of CO_2 (in kg). Since the vibrational levels are treated as separate species, only the heat capacity due to translational and rotational degrees of freedom and, in the case of CO_2, also the heat capacity due to the symmetric vibrational modes, which are not treated as individual species, should be taken into account [10,11]. A classical partitioning between the translational and rotational degrees of

freedom is assumed, which gives a value for the specific heat ratio, at room temperature and above, of 1.67 for the atomic species and 1.40 for the diatomic molecules . For O_3, a value of 1.27 was taken [10,12]. Details about the calculation of the total heat capacity and the resulting specific heat ratio for CO_2, calculated using equation (10), can be found in [10].

Table S.1: Electron impact reactions calculated with cross sections data, using the calculated EEDF, as explained in section 2.1 of the main paper, as well as the references where the data are adopted from.

No.	Reaction	Ref	Note
$(X1)^a$	$e^- + \ CO_2 \rightarrow 2e^- + CO_2^+$	[13–15]	
$(X2)^a$	$e^- + \ CO_2 \rightarrow 2e^- + O + CO^+$	[13–15]	
$(X3)^a$	$e^- + \ CO_2 \rightarrow 2e^- + O^+ + CO$	[16]	
$(X4)^a$	$e^- + \ CO_2 \rightarrow 2e^- + O_2 + C^+$	[16]	
$(X5)^a$	$e^- + \ CO_2 \rightarrow 2e^- + O_2^+ + C$	[17]	
$(X6)^a$	$e^- + \ CO_2 \rightarrow O^- + CO$	[13–15]	
$(X7)^b$	$e^- + \ CO_2 \rightarrow e^- + O + CO$	[13–15]	
$(X8)^a$	$e^- + \ CO_2 \rightarrow e^- + CO_2(E1)$	[13–15]	
$(X9)^b$	$e^- + \ CO_2 \leftrightarrow e^- + CO_2(Vx)$	[13–15]	$x = a, b, c, d$
$(X10)^c$	$e^- + \ CO_2 \leftrightarrow e^- + CO_2(Vi)$	[13–15]	$i = 1 - 21$
$(X11)^a$	$e^- + \ CO \rightarrow 2e^- + CO^+$	[18]	
$(X12)^a$	$e^- + \ CO \rightarrow 2e^- + C^+ + O$	[19]	
$(X13)^a$	$e^- + \ CO \rightarrow 2e^- + C + O^+$	[19]	
$(X14)^a$	$e^- + \ CO \rightarrow C + O^-$	[20]	
$(X14bis)^b$	$e^- + \ CO \rightarrow e^- + C + O$	[21]	
$(X15)$	$e^- + \ CO \leftrightarrow e^- + CO(Vi)$	[21]	$i = 1 - 10$
$(X16)^b$	$e^- + \ O_2 \rightarrow e^- + O + O$	[22]	

$(X16M)^a$	$e^- + O_2 + M \rightarrow O_2^- + M$	[22]	
$(X17)^a$	$e^- + O_2 \rightarrow O + O^-$	[22]	
$(X18)^a$	$e^- + O_2 \rightarrow 2e^- + O_2^+$	[23]	
$(X19)^b$	$e^- + O_2 \rightarrow 2e^- + O + O^+$	[23]	
$(X20)$	$e^- + O_2 \leftrightarrow e^- + O_2(Vi)$	[22]	$i = 1,2,3,4$
$(X21)$	$e^- + O_3 \rightarrow e^- + O_2 + O$	[24]	
$(X22)$	$e^- + O_3 \rightarrow 2e^- + O_2^+ + O$	[24]	
$(X23)$	$e^- + O_3 \rightarrow e^- + O^+ + O^- + O$	[24]	
$(X24)$	$e^- + O_3 \rightarrow O^- + O_2$	[25]	
$(X25)$	$e^- + O_3 \rightarrow O + O_2^-$	[25]	
$(X26)$	$e^- + O \rightarrow 2e^- + O^+$	[26]	
$(X27)$	$e^- + C \rightarrow 2e^- + C^+$	[27]	

[a] Same cross section also used for ground state.

[b] Cross section also used for the excited states, modified by lowering the energy threshold by the energy of the excited state.

[c] Cross section for the various levels (i,j) adopted from $e^- + CO_2 \rightarrow e^- + CO_2(Vi)$ but scaled and shifted using Fridman's approximation [28,29]

Table S.2: Electron impact reactions using analytical expressions for the rate coefficients, given in $m^3\ s^{-1}$ and $m^6\ s^{-1}$, for two-body and three-body reactions, respectively, as well as the references where the data are adopted from. T_g and T_e are given in K and eV, respectively.

No.	Reaction	Rate coefficient	Ref
$(E1a)$	$e^- + CO_2^+ \rightarrow CO(V1) + O$	$1.0x10^{-11}T_e^{-0.5}T_g^{-1}$	[30,31]
$(E1b)$	$e^- + CO_2^+ \rightarrow C + O_2$	$1.0x10^{-11}T_e^{-0.5}T_g^{-1}$	[17]
$(E2)^a$	$e^- + CO_4^+ \rightarrow CO_2 + O_2$	$1.61x10^{-13}T_e^{-0.5}$	[17]

$(E3)$	$e^- + \ CO^+ \rightarrow C + O$	$3.46x10^{-14}T_e^{-0.48}$	[32,33]
$(E4)^a$	$e^- + \ O + M \rightarrow O^- + M$	$1.0x10^{-43}$	[31]
[a] The primary source was not accessible			

Table S.3: Ion-ion and ion-neutral reactions, as well as the references where the data are adopted from. The rate coefficients are given in $m^3\ s^{-1}$ and $m^6\ s^{-1}$, for two-body and three-body reactions, respectively. T_g is given in K.

No.	Reaction	Rate coefficient	Ref
$(I1)$	$CO_2 + CO^+ \rightarrow CO_2^+ + CO$	$1.0x10^{-15}$	[34,35]
$(I2)$	$CO_2 + O^- + M \rightarrow CO_3^- + M$	$1.5x10^{-40}$	[34,36]
$(I3)$	$CO_2 + O_2^- + M \rightarrow CO_4^- + M$	$4.7x10^{-41}$	[34,36]
$(I4)$	$CO + O^- \rightarrow CO_2 + e^-$	$5.5x10^{-16}$	[34,37]
$(I5)$	$CO + CO_3^- \rightarrow 2CO_2 + e^-$	$5.0x10^{-19}$	[38]
$(I6)^a$	$CO_3^- + CO_2^+ \rightarrow 2CO_2(Vb) + O$	$5.0x10^{-13}$	[31]
$(I7)^a$	$CO_4^- + CO_2^+ \rightarrow 2CO_2(Vb) + O_2$	$5.0x10^{-13}$	[31]
$(I8)^a$	$O_2^- + CO_2^+ \rightarrow CO_2(V1) + O_2 + O$	$6.0x10^{-13}$	[31]
$(I9)$	$CO_3^- + O \rightarrow CO_2 + O_2^-$	$8.0x10^{-17}$	[39]
$(I10a)^a$	$CO_4^- + O \rightarrow CO_3^- + O_2$	$1.12x10^{-16}$	[34]
$(I10b)^a$	$CO_4^- + O \rightarrow CO_2 + O_2 + O^-$	$1.4x10^{-17}$	[34]
$(I11)$	$O + O^- \rightarrow O_2 + e^-$	$2.3x10^{-16}$	[40]
$(I12)^a$	$O + O_2^- \rightarrow O_2 + O^-$	$1.5x10^{-16}$	[34]
$(I13)$	$O_2^- + M \rightarrow O_2 + M + e^-$	$2.7x10^{-16}(\frac{T_g}{300})^{0.5}\exp(-5590/T_g)$	[41,42]
$(I14)^c$	$O^- + M \rightarrow O + M + e^-$	$2.3x10^{-15}\exp(-26000/T_g)$	[42–44]

[a] The primary source was not accessible

[c] For usual values of gas temperature, i.e. T_g<< 26,000 K, the rate coefficient is very low, as pointed out by Gudmundsson[45].

Table S.4: : Neutral-neutral reactions, as well as the references where the data are adopted from. The rate coefficients are given in m^3 s^{-1} and m^6 s^{-1}, for two-body and three-body reactions, respectively. T_g is given in K. The α parameter determines the effectiveness of lowering the activation energy for reactions involving vibrationally excited levels of the molecules (see details in [28,29])

No.	Reaction	Rate coefficient	α	Ref
$(N1)$	$CO_2 + M \rightarrow CO + O + M$	$6.06x10^{-16}\exp(-52525/T_g)$	0.82	[46]
$(N2)$	$CO_2 + O \rightarrow CO + O_2$	$2.8x10^{-17}\exp(-26500/T_g)$	0.50	[47,48]
$(N3)$	$CO_2 + C \rightarrow 2CO$	$< 1.0x10^{-21}$	n.a.	[49]
$(N4)$	$CO + O + M \rightarrow CO_2 + M$	$8.3x10^{-46}\exp(-1510/T_g)$	0.0	[48,50]
$(N5)$	$O_2 + CO \rightarrow CO_2 + O$	$4.2x10^{-18}\exp(-24000/T_g)$	0.5	[48]
$(N6)$	$O_2 + C \rightarrow CO + O$	$1.99x10^{-16}\exp(-2010/T_g)$	0.0	[51]
$(N7)$	$O + C + M \rightarrow CO + M$	$2.14x10^{-41}\left(\frac{T_g}{300}\right)^{-3.08}\exp(-2144/T_g)$	0.0	[47,48]
$(N8)$	$O + O + M \rightarrow O_2 + M$	$5.2x10^{-47}\exp(900/T_g)$	n.a.	[47,48]
$(N9)$	$O_2 + M \rightarrow O + O + M$	$3.0x10^{-12}\frac{1}{T_g}\exp(-59380/T_g)$	1.0	[47,48]

Table S.5: Neutral reactions between vibrationally excited molecules, as well as the references where the data are adopted from. The rate coefficients are given in m^3 s^{-1} and m^6 s^{-1}, for two-body and three-body reactions, respectively. T_g is given in K.

No.	Reaction	Rate coefficient	Ref

$(V1)$	$CO_2(Va) + M \rightarrow CO_2 + M$	$7.14x10^{-15}\exp(-177T_g^{-1/3} + 451T_g^{-2/3})$	[52–54]
$(V2a)$	$CO_2(V1) + M \rightarrow CO_2(Va) + M$	$4.25x10^{-7}\exp(-407T_g^{-1/3} + 824T_g^{-2/3})$	[54–56]
$(V2b)$	$CO_2(V1) + M \rightarrow CO_2(Vb) + M$	$8.57x10^{-7}\exp(-404T_g^{-1/3} + 1096T_g^{-2/3})$	[54–56]
$(V2c)$	$CO_2(V1) + M \rightarrow CO_2(Vc) + M$	$1.43x10^{-7}\exp(-252T_g^{-1/3} + 685T_g^{-2/3})$	[54–56]
$(V3)$	$CO(V1) + M \rightarrow CO + M$	$1.0x10^{-18}T_g\exp(-150.7T_g^{-1/3})$	[57]
$(V4)$	$O_2(V1) + M \rightarrow O_2 + M$	$1.3x10^{-14}\exp(-158.7T_g^{-1/3})$	[53,54]
$(V5)$	$CO_2(V1) + CO_2 \rightarrow CO_2(Va) + CO_2(Vb)$	$1.06x10^{-11}\exp(-242T_g^{-1/3} + 633T_g^{-2/3})$	[54–56]
$(V6)$	$CO_2(V1) + CO_2 \rightarrow CO_2 + CO_2(V1)$	$1.32x10^{-18}\left(\frac{T_g}{300}\right)^{0.5}\frac{250}{T_g}$	[58,59]
$(V7)$	$CO(V1) + CO \rightarrow CO + CO(V1)$	$3.4x10^{-16}\left(\frac{T_g}{300}\right)^{0.5}(1.64x10^{-6}T_g + \frac{1.61}{T_g})$	[60,61]
$(V8)$	$CO_2(V1) + CO \rightarrow CO_2 + CO(V1)$	$4.8x10^{-12}\exp(-153T_g^{-1/3})$	[54,55]

2. Extra calculated plasma characteristics

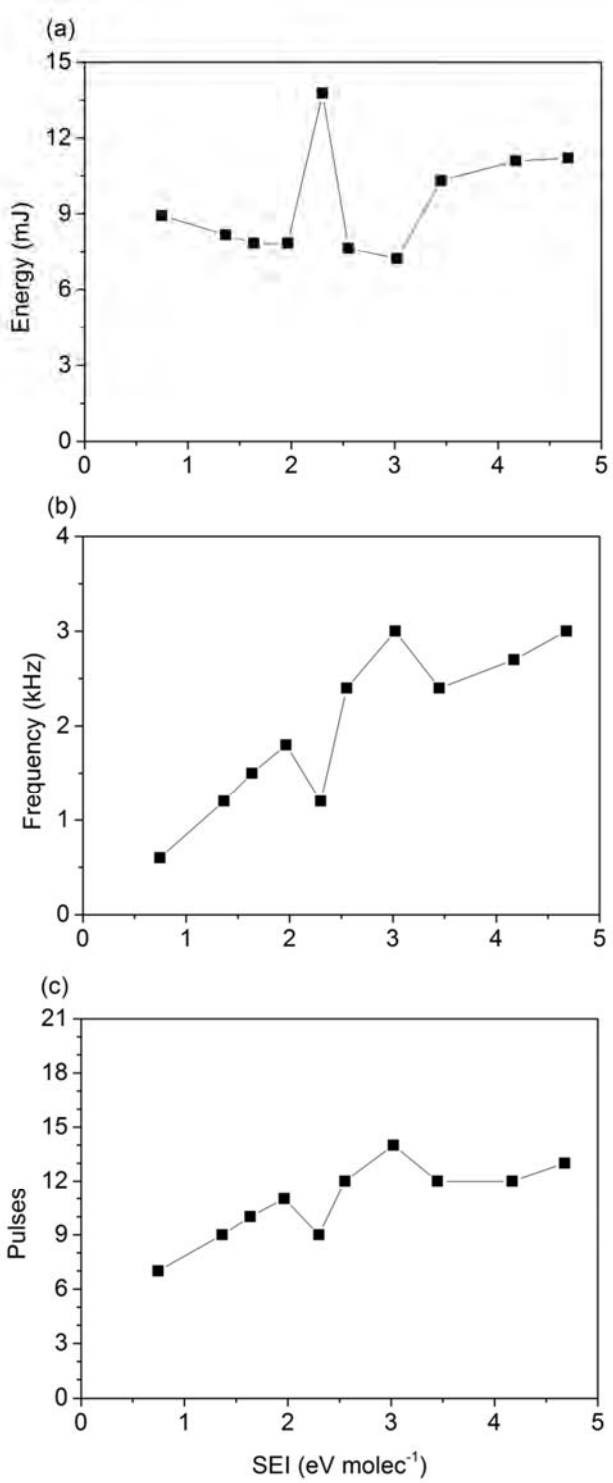

Figure S.1: Energy deposited per pulse (a), pulse frequency (b), and number of pulses felt by the gas molecules when travelling from pin HV electrode to grounded electrode (c), for the different SEI values investigated.

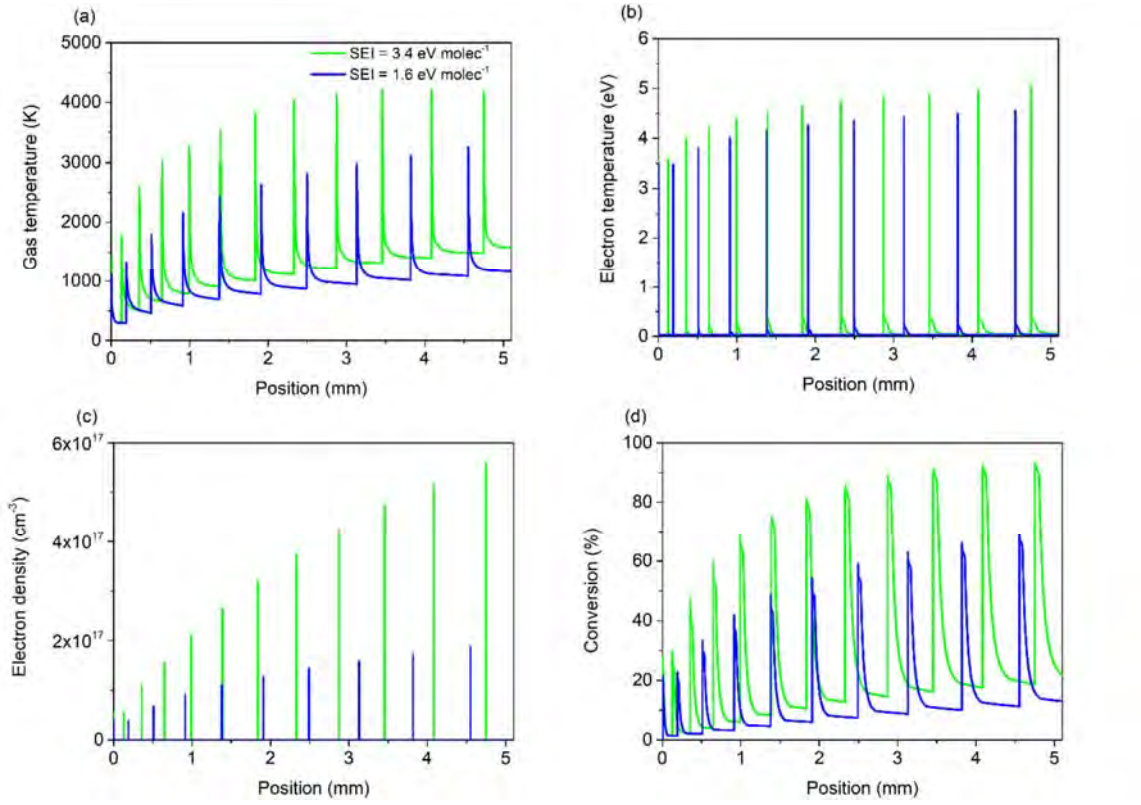

Figure S.2: Calculated gas temperature (a), electron temperature (b), electron density (c), and CO_2 conversion (d), as a function of travelled distance between HV pin electrode and grounded electrode, for two different SEI values (i.e. different from the SEI values in Figure 7 in the main paper, for extra information).

3. Details about the dissociation and formation mechanisms, and contribution of vibrational levels

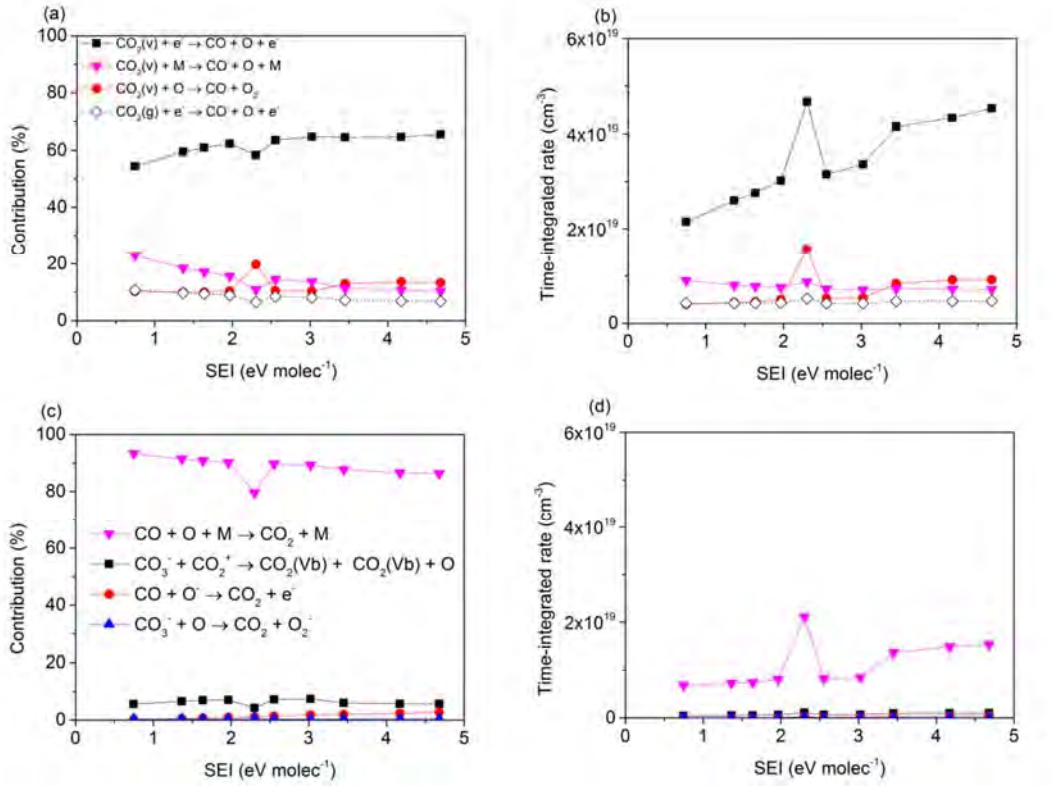

Figure S.3: Contribution of the most important dissociation (a) and formation (c) mechanisms of CO_2, and their corresponding time-integrated rates (b, d) as a function of SEI.

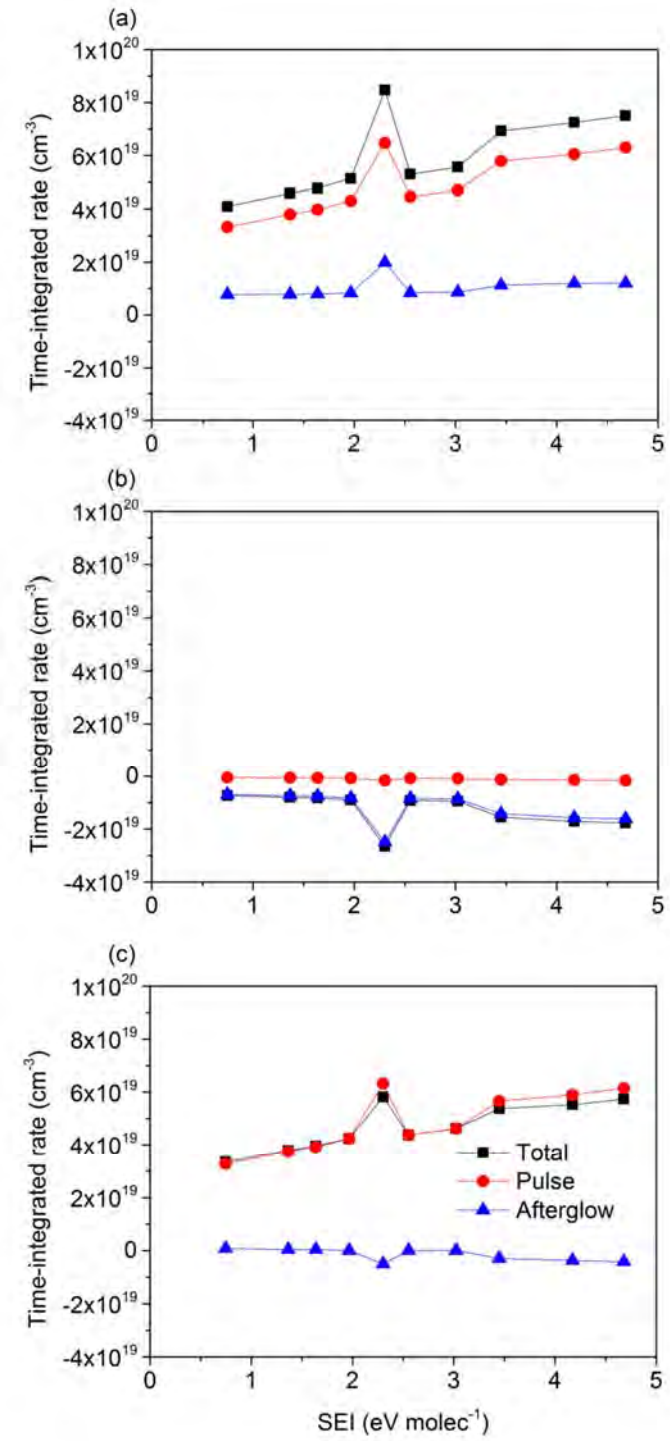

Figure S.4: Time-integrated rates of the overall dissociation (a), overall formation (plotted as negative values) (b), and the net dissociation of CO_2, as a function of SEI, for the pulse, afterglow and the sum of both (total), showing that the dissociation mainly takes place during the pulses, while net formation occurs during the afterglows.

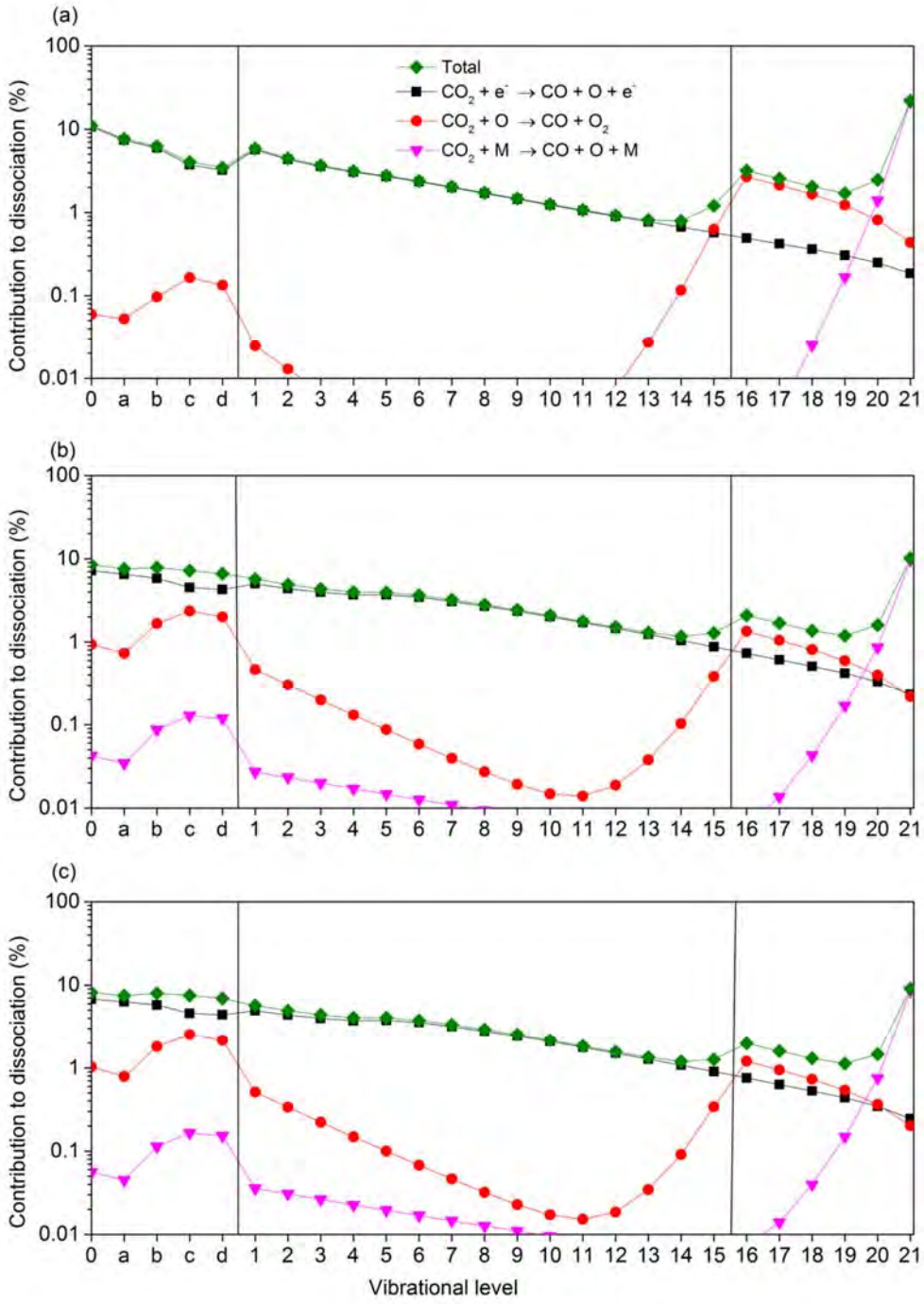

Figure S.5: Contribution of the CO_2 ground state and different vibrational levels to the total dissociation, as well as to the most important dissociation mechanisms, only accounting for the forward reactions, for different SEI values, i.e., 0.7 eV molec^{-1} (a), 3.4 eV molec^{-1} (b) and 4.7 eV molec^{-1} (c).

4. Details about the effect of cooling

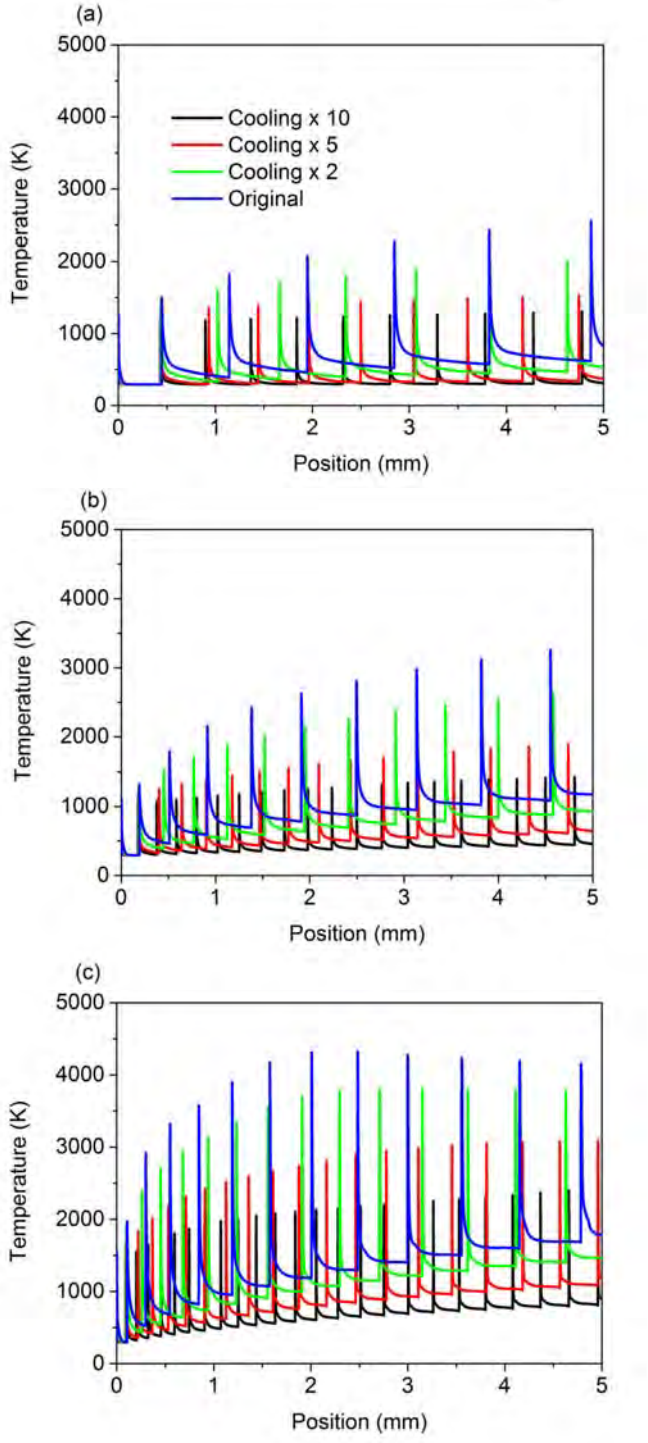

Figure S.6: Calculated gas temperature as a function of travelled distance between HV pin electrode and grounded electrode for different SEI values, i.e., 0.7 eV molec^{-1} (a), 1.6 eV molec^{-1} (b) and 4.7 eV molec^{-1} (c), at different cooling rates.

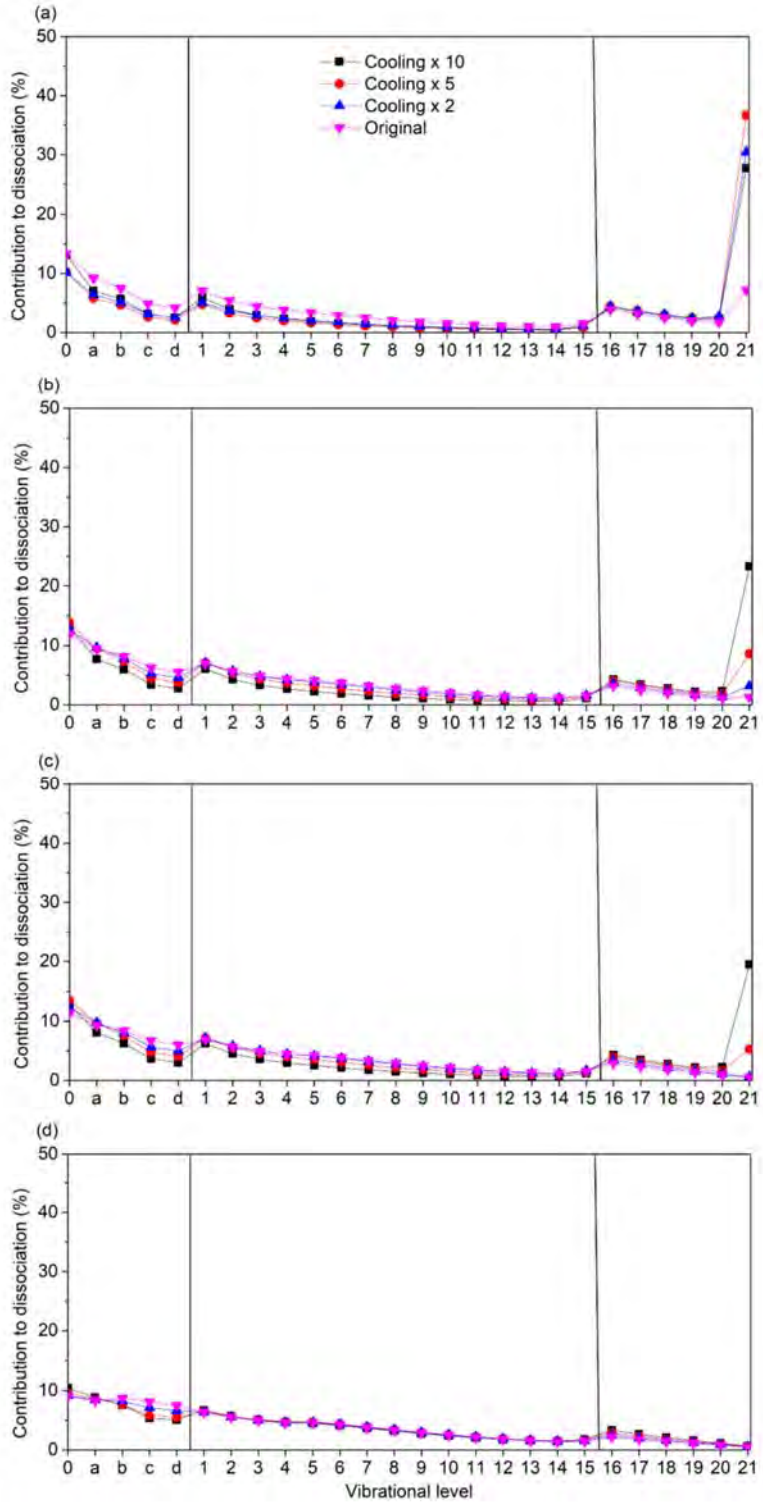

Figure S.7: Net contribution of the different CO_2 vibrational levels to the total dissociation, for different SEI values, i.e., 0.7 eV molec^{-1} (a), 1.6 eV molec^{-1} (b), 2.0 eV molec^{-1} (c) and 4.7 eV molec^{-1} (d), at different cooling rates.

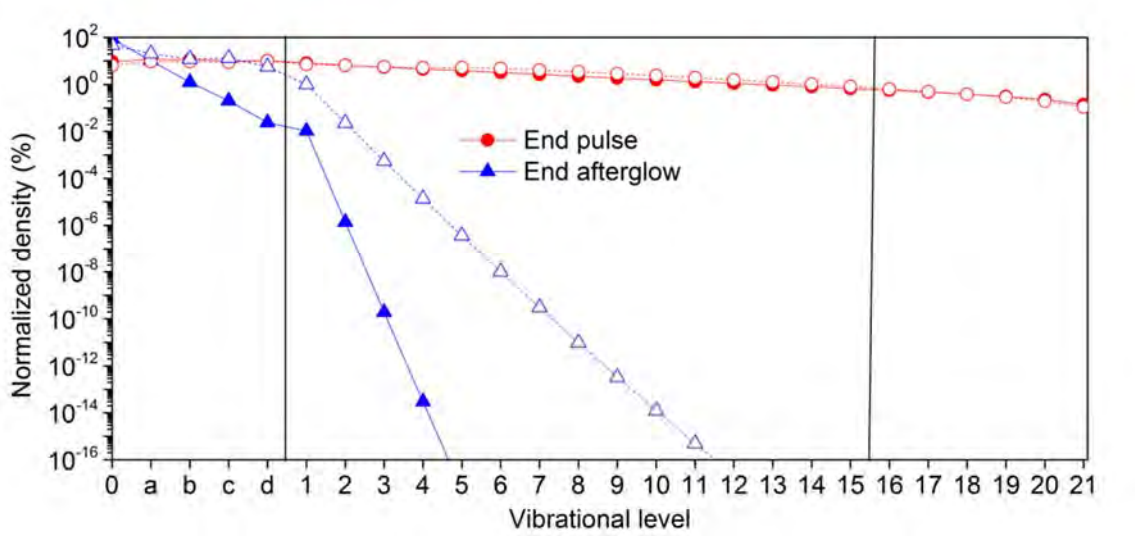

Figure S.8: Calculated VDFs at the end of the last pulse (10 ns) and at the end of the last afterglow, for SEI = 1.6 eV molec^{-1}, in the original model (open symbols, dashed lines) and with a cooling rate times ten (solid symbols and lines). The VDFs at cooling rate times two and five at the end of the pulse are the same, and at the end of the afterglow, they lie in between the VDFs of the original model and of ten times higher cooling rate.

5. References

(1) Pancheshnyi, S.; Eismann, B.; Hagelaar, G. J. M.; Pitchford, L. C. ZDPlasKin: A New Tool for Plasmachemical Simulations. University of Toulouse, LAPLACE, CNRS-UPS-INP, Toulouse, France, 2008, p University of Toulouse, LAPLACE, CNRS-UPS-INP.

(2) Hagelaar, G. J. M.; Pitchford, L. C. Solving the Boltzmann Equation to Obtain Electron Transport Coefficients and Rate Coefficients for Fluid Models. *Plasma Sources Sci. Technol.* **2005**, *14*, 722–733.

(3) Lieberman, M. A.; Lichtenberg, A. J. *Principles of Plasma Discharges and Materials Processing: Second Edition*, 2nd Editio.; Wiley-Interscience, 2005.

(4) Greig, J. R.; Pechacek, R. E.; Raleigh, M. Channel Cooling by Turbulent Convective Mixing. *Phys. Fluids* **1985**, *28*, 2357–2364.

(5) Shneider, M. N. Turbulent Decay of After-Spark Channels. *Phys. Plasmas* **2006**, *13*, 073501.

(6) Ramakers, M.; Trenchev, G.; Heijkers, S.; Wang, W.; Bogaerts, A. Gliding Arc Plasmatron: Providing a Novel Method for Carbon Dioxide Conversion. *Chem. Sus. Chem.* **2017**, *10*, 2642–2652.

(7) Cleiren, E.; Heijkers, S.; Ramakers, M.; Bogaerts, A. Dry Reforming of Methane in a Gliding Arc Plasmatron: Towards a Better Understanding of the Plasma Chemistry. *Chem. Sus. Chem.* **2017**, *10*, 4025–4036.

(8) Heijkers, S.; Bogaerts, A. CO_2 Conversion in a Gliding Arc Plasmatron: Elucidating the Chemistry through Kinetic Modeling. *J. Phys. Chem. C* **2017**, *121*, 22644–22655.

(9) Trenchev, G.; Kolev, S.; Wang, W.; Ramakers, M.; Bogaerts, A. CO_2 Conversion in a Gliding Arc Plasmatron: Multidimensional Modeling for Improved Efficiency. *J. Phys. Chem. C* **2017**, *121*, 24470–24479.

(10) Kozak, T.; Bogaerts, A. Evaluation of the Energy Efficiency of CO_2 Conversion in Microwave Discharges Using a Reaction Kinetics Model. *Plasma Sources Sci. Technol.* **2015**, *24*, 015024.

(11) Wang, W.; Berthelot, A.; Kolev, S.; Tu, X.; Bogaerts, A. CO_2 Conversion in a Gliding Arc Plasma: 1D Cylindrical Discharge Model. *Plasma Sources Sci. Technol.* **2016**, *25*, 065012.

(12) Chase, M. NIST-JANAF Thermochemical Tables, 4th Edition. *Journal of Physical and Chemical Reference Data, Monograph 9*. 1998, p 1952.

(13) Phelps, A. V. Phelps Database www.lxcat.net.

(14) Lowke, J. J.; Phelps, A. V.; Irwin, B. W. Predicted Electron Transport Coefficients and Operating Characteristics of CO_2/N_2/He Laser Mixtures. *J. Appl. Phys.* **1973**, *44*, 4664–4671.

(15) Hake, R. D.; Phelps, A. V. Momentum-Transfer and Inelastic-Collision Cross Sections for Electrons in O_2, CO, and CO_2. *Phys. Rev.* **1967**, *158*, 70–84.

(16) Itikawa, Y. Cross Sections for Electron Collisions with Carbon Dioxide. *J. Phys. Chem. Ref. Data* **2002**, *31*, 749–767.

(17) Beuthe, T. G.; Chang, J.-S. Chemical Kinetic Modelling of Non-Equilibrium Ar- CO_2 Thermal Plasmas. *Jpn. J. Appl. Phys.* **1997**, *36*, 4997–5002.

(18) Tian, C.; Vidal, C. R. Cross Sections of the Electron Impact Dissociative Ionization of CO, CH_4 and C_2H_2. *J. Phys. B At. Mol. Opt. Phys.* **1998**, *31*, 895–909.

(19) Itikawa, Y. Cross Sections for Electron Collisions with Carbon Monoxide. *J. Phys. Chem. Ref. Data* **2015**, *44*, 013105.

(20) Rapp, D.; Briglia, D. D. Total Cross Sections for Ionization and Attachment in Gases by Electron Impact. II. Negative-Ion Formation. *J. Chem. Phys.* **1965**, *43*, 1480–1489.

(21) Land, J. E. Electron Scattering Cross Sections for Momentum Transfer and Inelastic Excitation in Carbon Monoxide. *J. Appl. Phys.* **1978**, *49*, 5716–5721.

(22) Lawton, S. A.; Phelps, A. V. Excitation of the b 1Σ+g State of O_2 by Low Energy Electrons. *J. Chem. Phys.* **1978**, *69*, 1055–1068.

(23) Itikawa, Y. Cross Sections for Electron Collisions with Oxygen Molecules. *J. Phys. Chem. Ref. Data* **2009**, *38*, DOI: 10.1063/1.3025886.

(24) Eliasson, B.; Kogelschatz, U. *Basic Data for Modelling of Electrical Discharges in Gases: Oxygen*; Baden: ABB Asea Brown Boveri, 1986.

(25) Matejcik, S.; Kiendler, A.; Cicman, P.; Skalny, J.; Stampfli, P.; Illenberger, E.; Chu,

Y.; Stamatovic, A.; Märk, T. D. Electron Attachment to Molecules and Clusters of Atmospheric Relevance: Oxygen and Ozone. *Plasma Sources Sci. Technol.* **1997**, *6* (2), 140–146.

(26) Laher, R. R.; Gilmore, F. R. Updated Excitation and Ionization Cross Sections for Electron Impact on Atomic Oxygen. *J. Phys. Chem. Ref. Data* **1990**, *19*, 277–305.

(27) Morgan, W. L. Morgan Database Www.Lxcat.Net. *(retrieved 1 December 2015)*.

(28) Fridman, A. *Plasma Chemistry*; Cambridge University Press: New York, U.S.A., 2008.

(29) Kozák, T.; Bogaerts, A. Splitting of CO_2 by Vibrational Excitation in Non-Equilibrium Plasmas: A Reaction Kinetics Model. *Plasma Sources Sci. Technol.* **2014**, *23*, 045004.

(30) Weller, C. S.; Biondi, M. A. Measurements of Dissociative Recombination of CO_2^+ Ions with Electrons. *Phys. Rev. Lett.* **1967**, *19*, 59–61.

(31) Thoenes, J.; Kurzius, S. C. *Plasma Chemistry Processes in the Closed Cycle EDL-Technical Report DRCPMHEL-CR-79-11-VOL-1*; 1979.

(32) Mitchell, J. B. A.; Hus, H. The Dissociative Recombination and Excitation of CO+. *J. Phys. B At. Mol. Phys.* **1985**, *18*, 547–555.

(33) McElroy, D.; Walsh, C.; Markwick, A. J.; Cordiner, M. A.; Smith, K.; Millar, T. J. The UMIST Database for Astrochemistry 2012. *Astron. Astrophys.* **2012**, *550*, A36.

(34) Albritton, D. L. Ion-Neutral Reaction-Rate Constants Measured in Flow Reactors Through 1977. *At. Data Nucl. Data Tables* **1978**, *22*, 1–101.

(35) Adams, N. G.; Smith, D.; Grief, D. Reactions of H_nCO^+ Ions with Molecules at 300 K. *Int. J. Mass Spectrom. Ion Phys.* **1978**, *26*, 405–415.

(36) Fehsenfeld, F. C.; Ferguson, E. E. Laboratory Studies of Negative Ion Reactions with Atmospheric Trace Constituents. *J. Chem. Phys.* **1974**, *61*, 3181–3193.

(37) Mcfarland, M.; Albritton, D. L.; Fehsenfeld, F. C.; Ferguson, E. E.; Schmeltekopf, A. L. Flow-Drift Technique for Ion Mobility and Ion-Molecule Reaction Rate Constant Measurements. III. Negative Ion Reactions of O^- with CO, NO, H_2, and D_2. *J. Chem. Phys.* **1973**, *59*, 6629–6635.

(38) Price, D. A.; Moruzzi, J. L. Negative Ion Molecule Reactions in CO2 at High Pressures and Temperatures. *Vacuum* **1974**, *24*, 591–593.

(39) Fehsenfeld, F. C.; Schmeltekopf, A. L.; Schiff, H. I.; Ferguson, E. E. Laboratory Measurements of Negative Ion Reactions of Atmospheric Interest. *Planet. Space Sci.* **1967**, *15*, 373–379.

(40) Belostotsky, S. G.; Economou, D. J.; Lopaev, D. V.; Rakhimova, T. V. Negative Ion Destruction by $O(^3P)$ Atoms and $O_2(a\ ^1\Delta g)$ Molecules in an Oxygen Plasma. *Plasma Sources Sci. Technol.* **2005**, *14*, 532–542.

(41) Pack, J. L.; Phelps, A. V. Electron Attachment and Detachment. II. Mixtures of O_2 and CO_2 and of O_2 and H_2O. *J. Chem. Phys.* **1966**, *45*, 4316–4329.

(42) Bortner, M. H.; Bourer, T.; Blank, C. A. *Defense Nuclear Agency Reaction Rate*

Handbook, Second Edition AD 763699; 1972.

(43) Hasted, J. B.; Smith, R. A. The Detachment of Electrons from Negative Ions. *Proc. R. Soc. A Math. Phys. Eng. Sci.* **1956**, *235*, 349–353.

(44) Frommhold, L. Über Verzögerte Elektronen in Elektronenlawinen, Insbesondere in Sauerstoff Und Luft, Durch Bildung Und Zerfall Negativer Ionen (O-). *Fortschritte der Phys.* **1964**, *12*, 597–642.

(45) Gudmundsson, J. T. *A Critical Review of the Reaction Set for a Low Pressure Oxygen Processing Discharge RH-17-2004*; 2004.

(46) Burmeister, M.; Roth, P. ARAS Measurements on the Thermal Decomposition of CO_2. *AIAA J.* **1990**, *28*, 402–405.

(47) Baulch, D. L.; Drysdale, D. D.; Duxbury, J.; Grant, S. *Evaluated Kinetic Data for High Temperature Reactions, Volume 3: Homogeneous Gas Phase Reactions of the O_2-O_3 System, the CO-O_2-H_2 System, and of the Sulphur-Containing Species*; Butterworth, London, 1976.

(48) Tsang, W., R. F. H. Chemical Kinetic Data for Combustion Chemistry. Part 1. Methane and Related Compounds. *J. Phys. Chem. Ref. Data* **1986**, *15*, 1087–1279.

(49) Husain, D.; Young, A. N. Kinetic Investigation of Ground State Carbon Atoms, $C(2^3P_J)$. *J. Chem. Soc. Faraday Trans. 2* **1975**, *71*, 525.

(50) Baldwin, R. R.; Jackson, D.; Melvin, A.; Rossiter, B. N. The Second Limit of Hydrogen + Carbon Monoxide + Oxygen Mixtures. *Int. J. Chem. Kinet.* **1972**, *4*, 277–292.

(51) Dean, A. J.; Davidson, D. F.; Hanson, R. K. A Shock Tube Study of Reactions of C Atoms with H_2 and O_2 Using Excimer Photolysis of C_3O_2 and C Atom Atomic Resonance Absorption Spectroscopy. *J. Phys. Chem.* **1991**, *95*, 183–191.

(52) Simpson, C. J. S. M.; Chandler, T. R. D.; Strawson, A. C. Vibrational Relaxation in CO_2 and CO_2-Ar Mixtures Studied Using a Shock Tube and a Laser-Schlieren Technique. *J. Chem. Phys.* **1969**, *51*, 2214–2219.

(53) Taylor, R.; Bitterman, S. Survey of Vibrational Relaxation Data for Processes Important in the CO_2-N_2 Laser System. *Rev. Mod. Phys.* **1969**, *41*, 26–47.

(54) Blauer, J. A.; Nickerson, G. R. *A Survey of Vibrational Relaxation Rate Data For Processes Important To CO_2-N_2-H_2O Infrared Plume Radiation*; 1973.

(55) Rosser, W. A.; Wood, A. D.; Gerry, E. T. Deactivation of Vibrationally Excited Carbon Dioxide (v3) by Collisions with Carbon Dioxide or with Nitrogen. *J. Chem. Phys.* **1969**, *50*, 4996–5008.

(56) Herzfeld, K. F. Deactivation of Vibrations by Collision in the Presence of Fermi Resonance. *J. Chem. Phys.* **1967**, *47*, 743–752.

(57) Capitelli, M.; Ferreira, C. M.; Gordiets, B. F.; A.I., O. *Capitelli - Plasma Kinetics in Atmospheric Gases*; Springer(Berlin), 2000.

(58) Sharma, R. D. Near-Resonant Vibrational Energy Transfer Among Isotopes of CO_2.

Phys. Rev. **1969**, *177*, 102–107.

(59) Kreutz, T. G.; O'Neill, J. A.; Flynn, G. W. Diode Laser Absorption Probe of Vibration-Vibration Energy Transfer in CO_2. *J. Phys. Chem.* **1987**, *91*, 5540–5543.

(60) DeLeon, R. L.; Rich, J. W. Vibrational Energy Exchange Rates in Carbon Monoxide. *Chem. Phys.* **1986**, *107*, 283–292.

(61) Flament, C.; George, T.; Meister, K. A.; Tufts, J. C.; Rich, J. W.; Subramaniam, V. V.; Martin, J. P.; Piar, B.; Perrin, M. Y. Nonequilibrium Vibrational Kinetics of Carbon Monoxide at High Translational Mode Temperatures. *Chem. Phys.* **1992**, *163*, 241–262.